CONF-960493--19
UCRL-JC-123010

Far-field Radiation From a Cleaved Cylindrical Dielectric Waveguide

Charles Cerjan

This paper was prepared for submittal to the
Optical Society of America Extreme Ultraviolet Lithography
Boston, MA
April 29-May 3, 1996

July 9, 1996

Lawrence Livermore National Laboratory

DISCLAIMER

DISCLAIMER

Far-field Radiation From a Cleaved Cylindrical Dielectric Waveguide

C. Cerjan

Advanced Microtechnology Program, Lawrence Livermore National Laboratory, Livermore, CA 94550

July 09, 1996

Abstract

A determination of the angular spread in the far-field radiation pattern of a cleaved dielectric waveguide is made from the modal structure at the surface of the waveguide using the Smythe vector integral formulation. The essential features are the following. First, a mode exists in the fiber that has no wavelength cutoff – the so-called HE_{11} mode. This mode arises when non-azimuthal angular dependence of the incoming radiation is present. Second, the energy flow from this hybrid mode fills the fiber face and is not annularly shaped as opposed to the symmetric TE and TM modes. Third, the HE_{11} mode is not polarization dependent in contrast to the TE and TM modes. Fourth, for small differences in the indices of refraction between the core and cladding regions only the HE_{11} mode will be supported until the next modes appear around 3.33λ. At this point, three new modes can propagate and the modal structure of the radiation becomes more complicated. Fifth, the far-field radiation pattern will have negligibly small angular dependence in the phases of the vector fields when only the lowest mode is present; the amplitude has an overall angular dependent form factor. Furthermore, when other modes are present (above 3.33λ), the phase of the vector fields will acquire an angular dependence.

1. Introduction

The investigation of the modal structure of the propagated radiation in a fiber optic is relevant to the performance of a recently proposed interferometer[1]. The effective limitations of this interferometer's performance are dictated by the angular deviation of the far-field radiation pattern arising from the cleaved surface of a cylindrical dielectric fiber optic. Thus it is important to obtain estimates of this angular phase deviation given the specific materials and geometry relevant to this application.

The modal structure in a dielectric cylinder is typically treated in the limit of vanishingly small difference between the core and cladding indices of refraction[2],[3]. In this limit, many of the modes become degenerate and have cutoff frequencies at the zeros of the integral-order Bessel functions. A more complete investigation, without the limitations of the asymptotic theories, exists[4] but has not been used in subsequent research, possibly because of numerical concerns. This latter approach has been implemented to provide a determination of the fiber optic modes for arbitrary differences in the refractive indices between the core and cladding regions of the fiber optic.

With an evaluation of the modal structure in hand, the far-field radiation pattern from a perfectly cleaved face can be estimated using the Smythe vector formulation[5]. This formulation provides a mathematically and physically consistent framework for the far-field estimates, as opposed to the Kirchhoff formulation, using the modal structure at the cleaved surface as a boundary condition. The qualitative differences between the two theories is significant since the Kirchhoff approximation predicts only step-function changes in the phases of the fields – the phase information is trivial. The Smythe theory is not so limited and thus is more relevant to the proposed interferometric experimental design.

2. THEORETICAL BACKGROUND

In order to keep the discussion brief, the underlying theory of cylindrically symmetric wave guide propagation will not be repeated below. The important feature of the propagation within the fiber optic that should be borned in mind is that a hybrid mode exists which has no cutoff and thus propagates regardless of the core radius size. A rapid overview of this extension follows.

Following the standard treatment of Jackson[5] and Snitzer[4], the z-components of the incident radiation field are assumed, without loss of generality, to have the form

$$E_z = A_l J_l(u\rho/a)\cos(l\theta)\exp(i(hz-\omega t)) \qquad (1)$$

and

$$H_z = B_l J_l(u\rho/a)\sin(l\theta)\exp(i(hz-\omega t)) \qquad (2)$$

inside the core region. The functions $J_l(z)$ are the usual integral-order Bessel functions and ω is the frequency of the exciting radiation. The quantity h is the magnitude of the propagating wavevector within the wave guide that must, of course, be determined from material properties and boundary conditions. The fields in the cladding region are similar with the Bessel functions of the first kind replaced by the modified Hankel functions of the first kind, $K_l(z)$ and the amplitudes A_l and B_l replaced by C_l and D_l. The wave guide itself has dielectric constant ϵ_1 and radius a with a surrounding medium with dielectric ϵ_2.

The remaining field components – E_ρ, E_ϕ, H_ρ, and H_ϕ – are derived from the z-components after some manipulation of Maxwell's equations[5]. The continuity of the tangential components at $\rho = a$ then provides a set of nonlinear equations relating the unknown amplitudes, A_l, B_l, C_l, and D_l. These relations can be reduced to the following equation[4]

$$(\eta_1 + \eta_2)(k_1^2\eta_1 + k_2^2\eta_2) = l^2h^2(1/u^2 + 1/w^2)^2 \ , \quad (3)$$

where $k_i^2 = \omega^2\epsilon_i$, $\eta_1 = J_l'(u)/(uJ_l(u))$, and $\eta_2 = K_l'(w)/(wK_l(w))$. The remaining quantities are given by

$$u^2 = (k_1^2 - h^2)a^2 \quad (4)$$

and

$$w^2 = (h^2 - k_2^2)a^2 \ . \quad (5)$$

In general, radiation cannot propagate at arbitrary values of the core radius. The modal structure will have cutoff frequencies, or equivalently, cutoff wavelengths. By taking the limit $w \rightarrow 0$ in the above equations, these cutoff values can be determined as a function of angular order. The modes for $l = 0$ (azimuthal symmetry) are special since in this case the modes are purely transverse electric (TE) or transverse magnetic (TM). Nonzero values lead to hybrid modes in which all field components are nonvanishing. These hybrid modes are designated HE or EH modes corresponding to dominant H-field components (HE) or E-field components (EH).

In general, the cutoffs are determined by the following relations. The cutoff for $l = 0$ is given by $J_l(u) = 0$, that is, by the zeros of the zeroth order Bessel function. There are an infinite number of zeros to this equation leading to an infinite number of cutoff wavelengths. These cutoffs are designated either TM_{0m} or TE_{0m} where $m = 1, 2, \ldots$ label the roots. The cutoffs for $l = 1$ are determined by the relation $J_1(u) = 0$ and are similarly labeled as HE_{1m} and EH_{1m}. It should be noted that the case HE_{11} is special since it corresponds to the "trivial" root of J_1 at zero. A non-trivial solution to the matching conditions exists for this case and it represents a mode that propagates without a cutoff wavelength. The conditions for $l \geq 2$ are $J_l(u) = 0$ for EH_{lm} and

$$\frac{uJ_{l-2}(u)}{J_{l-1}(u)} = -(l-1)\frac{(\epsilon_1 - \epsilon_2)}{\epsilon_2} \quad (6)$$

for HE_{lm}.

The vector fields present in the core and cladding can be parametrized by a quantity termed P in Snitzer where

$$P = \frac{l(1/u^2 + 1/w^2)}{\eta_1 + \eta_2} \ . \quad (7)$$

The field components are then given by

$$E_z = J_l(u\rho/a)F_c \quad (8)$$

$$E_\rho = i\frac{ha}{u}\left(\frac{1-P}{2}J_{l-1} - \frac{1+P}{2}J_{l+1}\right)F_c \quad (9)$$

$$E_\phi = -i\frac{ha}{u}\left(\frac{1-P}{2}J_{l-1} + \frac{1+P}{2}J_{l+1}\right)F_s \quad (10)$$

$$H_z = -\frac{\lambda ha}{2\pi}PJ_l(u\rho/a)F_s \quad (11)$$

$$H_\rho = i\frac{\lambda k_1^2 a}{2\pi u}\left(\frac{1-Ph^2/k_1^2}{2}J_{l-1} + \frac{1+Ph^2/k_1^2}{2}J_{l+1}\right)F_s \quad (12)$$

$$H_\phi = i\frac{\lambda k_1^2 a}{2\pi u}\left(\frac{1-Ph^2/k_1^2}{2}J_{l-1} - \frac{1+Ph^2/k_1^2}{2}J_{l+1}\right)F_c \ . \quad (13)$$

The field values in the cladding region are similar with the ordinary Bessel functions replaced by the modifed ones and the quantity w replaces u. The overall phase factor, F_c is

$$F_c = A_l\cos(l\phi)\exp(i(hz - \omega t)) \ , \quad (14)$$

and F_s is the same with $\sin(l\phi)$ replacing the cosine. The energy flow through the fiber optic is given by the Poynting vector, which in this particular geometry is given solely by the transverse fields

$$S_z = \frac{1}{2}(E_\rho H_\phi - E_\phi H_\rho) \ . \quad (15)$$

The far-field radiation expected from a perfectly cleaved dielectric wave guide can be calculated using the Smythe formulation[5]. This formulation uses an integral equation technique for the vector field components restricted to a two-dimensional surface. In the case of interest here, that two-dimensional surface is the plane of the fiber optic face. The cladding region contribution can also be calculated by a simple extension of this integral equation approach[6]. Estimates of the cladding contribution indicated that these external effects have an insignificant effect on the far-field radiation pattern since they are either small in amplitude or possess the same angular phase deviation as the core contributions.

More specifically, the resolvent of the integral equation, e^{ikR}/R with $R = ((z-z_0)^2+(\rho-\rho_0)^2-2\rho\rho_0\cos(\phi-\phi_0))^{1/2}$, can be expanded in some suitable co-ordinate system; the wave guide modes are used on the fiber optic face; and the resultant far-field patterns are calculated by taking overlap integrals between the wave guide modes and the resolvent expansion over the core region. The resolvent has the form

$$\frac{e^{ikR}}{R} = 4\pi i \sum_{l=0}^{\infty} j_l(kr_0)h_l^{(1)}(kr) \sum_{m=-l}^{l} Y_{lm}^*(\theta_0,\phi_0)Y_{lm}(\theta,\phi) \tag{16}$$

where j_l is a spherical Bessel function of order l, $h_l^{(1)}$ is a spherical Hankel function of order l, and Y_{lm} is a spherical harmonic function. Since the wave guide modes have azimuthal variation given by $\cos(l\phi)$, this symmetry will persist in the far-field when angular projections are taken with the resolvent expansion.

In the far-field limit and assuming the lth wave guide mode, the various vector components will be determined by the expansion

$$E_{far} = 4\pi\frac{e^{ikr}}{kr}\cos(l\phi)\sum_{l'=0}^{\infty}(-i)^{l'}P_{l'}^{l}(\pi/2)P_{l'}^{l}(\theta)I_{l'}\,, \tag{17}$$

where the overlap integral, $I_{l'}$, is

$$I_{l'} = a^2\int_0^1 vJ_{l'\pm1}j_{l'}(akv)\,dv\,. \tag{18}$$

Two important features of this solution should be noted. First, the symmetry of each wave guide mode forces the far-field solution to have a completely real or completely imaginary factor multiplying the outgoing spherical wave form. Thus, when modes of different symmetry are available, say at larger core radii, then the outgoing spherical wave will have an angularly dependent phase factor. Second, in the optimal case of only one supported mode (the HE_{11} mode), the phase of the outgoing spherical wave will have no angular dependence but the amplitude will in both the ϕ and θ directions.

3. NUMERICAL RESULTS

The set of transcendental equations were solved by standard nonlinear root search routines using stabilized recurrence schemes for the Bessel functions. As a technical note, the root search was performed in two stages to ensure stability after the introduction of a special factorization. The various parameters were chosen to be the expected experimental values[1]. Specifically, the real index of refraction for the inner core was 1.4658, that of the cladding material was 1.4613. The wavelength of the incident light was chosen to be monochromatic at 0.5148 microns. The core region was assumed to have a radius of either $a = \lambda$ or $a = 2\lambda$ which restricts the solutions to the lowest mode. This choice simplifies the analysis and should correspond to the desired experimental conditions.

The numerically determined values of the cutoffs for the dielectric constant values assumed here are listed in Table 1 for $l = 0,1,2$ and $m = 1,2,3,4$. Two general comments can be made about the number of modes expected in the wave guide. First, the modes are well-separated for a small difference between the core and cladding dielectric constants, but as this difference grows the modes will coalesce. Second, for a fixed difference in dielectric constant, a large number of modes will be present as the radius of the core region increases. Thus single-mode operation of the wave guide demands a relatively small change in dielectric constant and small core radius.

Table 1. Minimum core radius for mode propagation.

$a(\lambda)$	*mode*
0.000	HE_{11}
3.334	TE_{01},TM_{01}
3.338	HE_{21}
5.314	HE_{12}, EH_{11}
7.212	EH_{21}
7.655	TE_{02},TM_{02}
7.656	HE_{22}
9.729	HE_{13}, EH_{12}
11.672	EH_{22}
12.000	TE_{03},TM_{03}
12.001	HE_{24}
14.108	HE_{14}, EH_{13}
16.114	EH_{23}
16.351	TE_{04},TM_{04}
16.352	HE_{25}
18.476	HE_{15}, EH_{14}
20.518	EH_{24}

The resulting fields were evaluated for the two choices of radius. The values of u determined for both λ and 2λ are respectively 0.719 and 1.287; the values of w are similarly 0.0498 and 0.651. These values correspond to propagation amplitudes of 9.182 and 18.375.

The amplitude of the Poynting vector for the two cases is plotted in Figures 1 and 2 as a function of radial distance from the origin in units of the incident wavelength. The results in Figure 1, for $a = \lambda$, indicate that the field persists well into the cladding region compared to the $a = 2\lambda$ case in Figure 2. In neither case, though, is the cladding contribution significant past 40λ. This result is used to justify the integration region chosen for the far-field determinations.

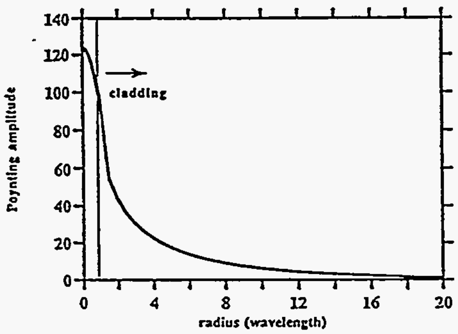

Fig. 1. Poynting vector amplitude as a function of the radius in units of the incident wavelength for a core radius of λ.

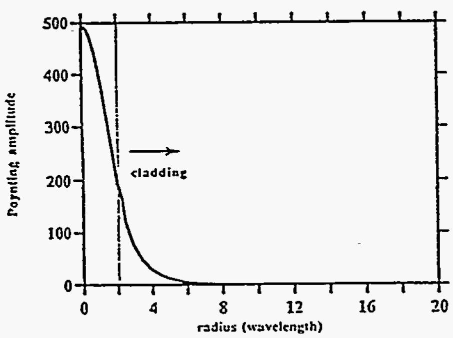

Fig. 2. Poynting vector amplitude as a function of the radius in units of the incident wavelength for a core radius of 2λ.

The far-field patterns were likewise determined using the approach outlined above. The requisite values of the parameter P and u were obtained assuming that the truncated fiber optic radiates with the interior modal structure. This boundary condition differs substantially from the case of a plane wave diffracting from a circular aperture. In the diffractive case, in a sense, all modes would be present. The wave guide acts a filter selecting only those components of the incident radiation that can propagate.

For the radii and dielectric constants chosen, the only mode that can propagate is the lowest mode, HE_{11}. The results obtained are plotted in Figures 3 - 6 for the angular form factors of the vector fields as a function of the opening angle, θ, away from the axis of the fiber optic. Recall from the above discussion that the phase of this one isolated mode is purely real so that the angular dependence of the radiation is contained in an overall real form-factor modulating the amplitudes of the E and H fields. That is,

$$E_{far} = 4\pi \frac{e^{ikr}}{kr} f_E(\theta) F_t \, , \tag{19}$$

and

$$H_{far} = 4\pi \frac{e^{ikr}}{kr} f_H(\theta) F_t \, , \tag{20}$$

where F_t represents either the cosine or sine function of $l\phi$, the azimuthal angle co-ordinate. Qualitatively, the trend is clear – the smaller radius fiber radiates into a larger far-field angle than the larger radius. Furthermore, the gradient of the angular form factors are approximately the same, about 0.0125 over a range of 16° in the angle θ.

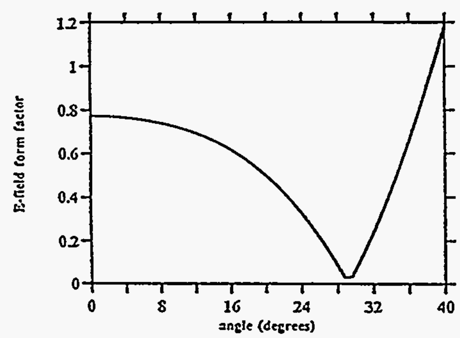

Fig. 3. Electric field form-factor as a function of the opening angle for a core radius of λ.

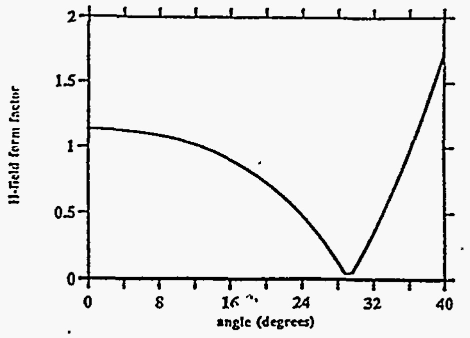

Fig. 4. Magnetic field form-factor as a function of the opening angle for a core radius of λ.

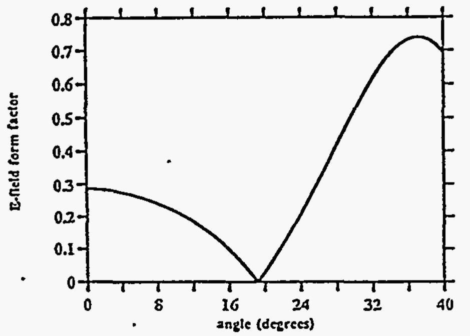

Fig. 5. Electric field form-factor as a function of the opening angle for a core radius of 2λ.

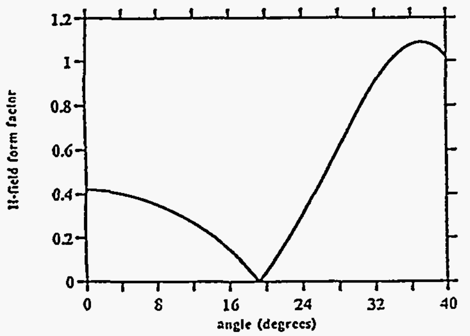

Fig. 6. Magnetic field form-factor as a function of the opening angle for a core radius of 2λ.

4. CONCLUSIONS

A methodology has been presented that can calculate the structure of the exact modal patterns expected inside a dielectric wave guide. These solutions can then be used to evaluate the far-field radiation distribution using the vector Smythe formulation. The primary conclusions are that by breaking the azimuthal symmetry of the assumed solutions, a mode is found that propagates without wavelength cutoff. This mode remains isolated until the TE_{01}, TM_{01}, and HE_{21} modes appear. The modal structure can then become a complicated mixture of hybrid modes. In the far-field, the original symmetry of the fiber optic mode persists in the radiation pattern. Furthermore, when only the lowest mode is present, only the amplitude of the fields are angularly modulated and not the phase. When modes of other symmetry appear, though, the phase will acquire an appreciable angular dependence.

ACKNOWLEDGMENTS

This work is performed under the auspices of the U. S. Department of Energy by the Lawrence Livermore National Laboratory under contract number W-7405-Eng-48.

1. G. E. Sommargren, "Phase-shifting diffraction interferometry for measuring EUV optics", presented at this conference.
2. A. W. Snyder, *IEEE Trans. Microwave Theory Techniques*, MTT-17, 1130(1969).
3. D. Gloge, *Appl. Opt.*, 10 2252(1971).
4. E. Snitzer, *J. Opt. Soc. Am.*, 51, 491(1961).
5. J. D. Jackson, "Classical Electrodynamics", 2nd edition, Chp. 9, (Wiley, New York, 1975).
6. C. Cerjan, unpublished results.